

## **SUPPLEMENTARY INFORMATION**

### **TARGETING OF MUCOLIPIN-1**

**Figure S1. The C-terminal di-leucine motif of mucolipin-1 is not sufficient for lysosomal targeting.** NRK cells stably expressing CD8-mucolipin-1 tail chimeras, wild type (wt) or double di-leucine to alanine mutant (L577/578A), were fixed and double-labelled with rat anti-CD8 (a gift from Dr G. Hale, Oxford University, UK; used as described (39)) and rabbit anti-Igp110 antibodies (38), followed by AlexaFluor 555- and AlexaFluor 488-conjugated secondary antibodies respectively. Merged confocal images show the extent of co-localisation between the chimeric proteins and Igp110. cDNAs encoding the CD8-mucolipin-1 tail chimeras were cloned into  $\Delta$ pMEP4. Bars, 10  $\mu$ m.

### **CHARACTERISATION OF MLIV FIBROBLASTS**

The MCOLN1 gene in the MLIV cells used in the present study has been characterized previously (3), with each parent having a different heterozygous mutation (WG0987 lacks exons 1-6 of MCOLN1; WG0988 has an A to G mutation resulting in the skipping of exon 4; WG0909 is the compound heterozygote of these mutations).

To characterise the fibroblasts, before undertaking the glycosphingolipid traffic rescue experiments, we used transmission electron microscopy to show that the patient's cells but not the parental cells had the classical morphology of MLIV cells (40) and contained swollen late endocytic organelles (lysosomes) filled with multi-concentric lamellae. We also determined the luminal pH of these organelles because of conflicting reports that it was either elevated by  $\sim$ 1pH unit (32), normal (33), or reduced (9) in fibroblasts from other MLIV patients. Because of the significant but variable autofluorescence of late endocytic organelles in the MLIV patient's cell (31)

we used a flow cytometry method (41). Cells were pulse-chased (4 h pulse, 20 h chase) with both fluorescein dextran (FD) which has pH-dependent fluorescence and Alexa Fluor 647 dextran (AF647D) which has pH-independent fluorescence. Under these culture conditions the dextran compartmentalises to lysosomes in normal fibroblasts (14,16). Ratiometric measurements of FD and AF647D were then made in the patient's and parents' cells and the pH of the lysosomes calculated from a standard curve as previously described (42). The mean lysosomal pH for WG0909 was pH  $5.07 \pm 0.26$ ; WG0987, pH  $4.87 \pm 0.29$  and WG0988, pH  $5.12 \pm 0.29$  (data are means  $\pm$  SEM, n=3) showing no significant difference between the patient's and parents' cells.

#### **ALIGNMENT OF PORE REGIONS**

The alignment of part of the pore region of human mucolipin-1 (Muc-1) with members of the TRP super-family and a voltage-gated  $\text{Ca}^{2+}$  channel, CACNLIA1 shown on Fig 5A used published sequence information (43-47).

#### **ELECTROPHYSIOLOGY OF MUCOLIPIN-1**

##### **Figure S2. Electrophysiology recordings in *Xenopus* oocytes and HEK-293 cells.**

(A-G) cDNAs encoding GFP-mucolipin-1 and the double di-leucine mutated GFP-mucolipin-1 (L15/16A + L577/578A) were cloned into pBF which provides 5' and 3' untranslated regions from the *Xenopus*  $\beta$ -globin gene (48). Capped RNA was synthesised using a mMESSAGE mMACHINE™ SP6 kit (Ambion, Europe, Ltd, UK), purified using MEGAclean™ columns and injected into oocytes (48). (A) Total membranes (48) from oocytes injected with water (Ctrl), cRNA encoding GFP-mucolipin-1 (WT) or GFP-mutant mucolipin-1(L15/16A + L577/578A) were immunoblotted for GFP (arrowhead). (B-D) Oocytes injected with (B) water, (C) cRNA encoding GFP-mucolipin-1, or (D) cRNA encoding GFP-mutant mucolipin-

1(L15/16A + L577/578A) were fixed after removal of the vitelline membrane (49), 5µm frozen sections cut and green epi-fluorescence visualised using a Zeiss Axioplan microscope. Bars 250µm. (E) Cell-attached current recordings made in oocytes injected with cRNA as in A. Slope conductance was calculated from the current response to voltage ramps between -100 and 0mV. Data are means ±SEM, n≥7. (F) Macroscopic current recordings made from giant inside-out patches excised from oocytes injected as in A, using 500kΩ electrodes with varying bath Ca<sup>2+</sup> concentrations and symmetrical ~150mM K<sup>+</sup>, 1.2mM Ca<sup>2+</sup> in the pipette (extracellular) solution. The free [Ca<sup>2+</sup>] in the bath was 40nM calculated with BAD4-software (50). Slope conductance calculated as in E. Data are means ±SEM, n≥4. (G) Macroscopic current recordings made from giant inside-out patches as in F but in the presence of 500 µM GTPγS or 250nM NAADP in the intracellular (bath) solution. Slope conductance calculated as in E. Data are means ±SEM, n≥3. (H-J). HEK-293 cells were transfected with either pEGFP-C3 (H) or a cDNA encoding the double dileucine mutated GFP-mucolipin-1 (L15/16A + L577/578A) in pEGFP-C3 (I) and stably transfected cells selected. (H) Green epifluorescence image of GFP cells, (I) green epifluorescence image of L15/16A + L577/578A cells. (J) Perforated patch whole cell conductance of GFP and L15/16A + L577/578A cells recorded in the presence of ~150mM Na<sup>+</sup>, 2mM Ca<sup>2+</sup> in the bath. Slope conductance was calculated from the current response to a voltage ramp between -80 and -20mV and was normalised for cell size. Data are means ±SEM, n≥13.

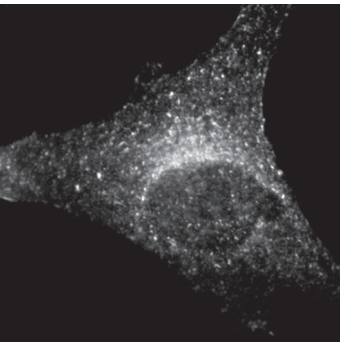
## **SUPPLEMENTARY REFERENCES**

39. Ihrke G, Gray SR, Luzio JP. Endolyn is a mucin-like type I membrane protein targeted to lysosomes by its cytoplasmic tail. *Biochem J* 2000; 345:287-296.

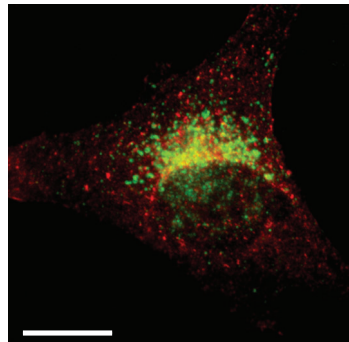
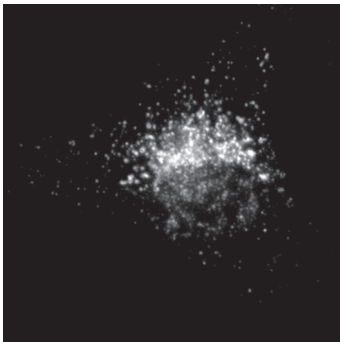
40. Kohn G, Livni N, Ornoy A, Sekeles E, Beyth Y, Legum C, Bach G, Cohen MM. Prenatal diagnosis of mucopolidosis IV by electron microscopy. *J Pediatr* 1977;90:62-66.
41. Rybak SL, Murphy RF. Primary cell cultures from murine kidney and heart differ in endosomal pH. *J Cell Physiol* 1998;176:216-222.
42. Bayer N, Schober D, Huttinger M, Blaas D, Fuchs R. Inhibition of clathrin-dependent endocytosis has multiple effects on human rhinovirus serotype 2 cell entry. *J Biol Chem* 2001;276:3952-3962.
43. Garcia-Martinez C, Morenilla-Palao C, Planells-Cases R, Merino JM, Ferrer-Montiel A. Identification of an aspartic residue in the P-loop of the vanilloid receptor that modulates pore properties. *J Biol Chem* 2000;275: 32552-32558.
44. Hoenderop JG, Voets T, Hoefs S, Weidema F, Prenen J, Nilius B, Bindels RJ. Homo- and heterotetrameric architecture of the epithelial Ca<sup>2+</sup> channels TRPV5 and TRPV6. *EMBO J* 2003;22: 776-785.
45. Nilius B, Vennekens R, Prenen J, Hoenderop JG, Droogmans G, Bindels RJ. The single pore residue Asp<sup>542</sup> determines Ca<sup>2+</sup> permeation and Mg<sup>2+</sup> block of the epithelial Ca<sup>2+</sup> channel. *J Biol Chem* 2001;276: 1020-1025.
46. Voets T, Prenen J, Vriens J, Watanabe H, Janssens A, Wissenbach U, Bodding M, Droogmans G, Nilius B. Molecular determinants of permeation through the cation channel TRPV4. *J Biol Chem* 2002; 277: 33704-33710.
47. Yang J, Ellinor PT, Sather WA, Zhang JF, Tsien RW. Molecular determinants of Ca<sup>2+</sup> selectivity and ion permeation in L-type Ca<sup>2+</sup> channels. *Nature* 1993;366:158-161.

48. Gribble FM, Ashfield R, Ammala C, Ashcroft FM. Properties of cloned ATP-sensitive K<sup>+</sup> currents expressed in *Xenopus* oocytes. *J Physiol* 1997;498: 87-98.
49. Roberson MM, Barondes SH. *Xenopus laevis* lectin is localized at several sites in *Xenopus* oocytes, eggs, and embryos. *J Cell Biol* 1983; 97: 1875-1881.
50. Brooks SP, Storey KB. Bound and determined: a computer program for making buffers of defined ion concentrations. *Anal Biochem* 1992;201: 119-126.

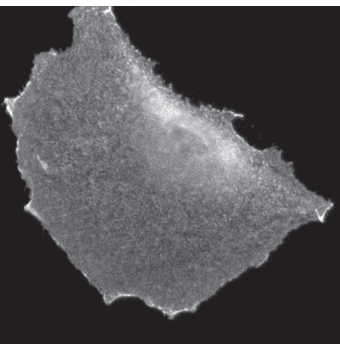
**CD8-mucolipin-1 (wt)**



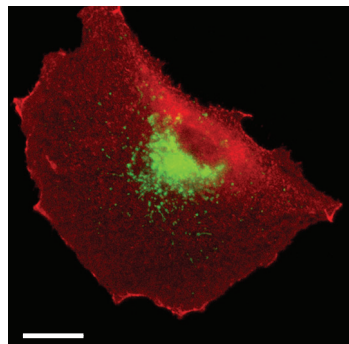
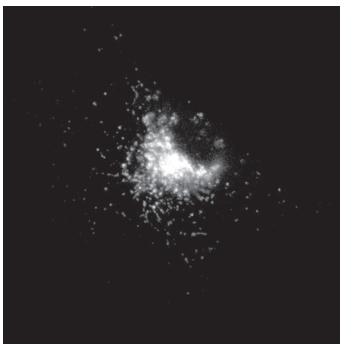
**Lgp110**



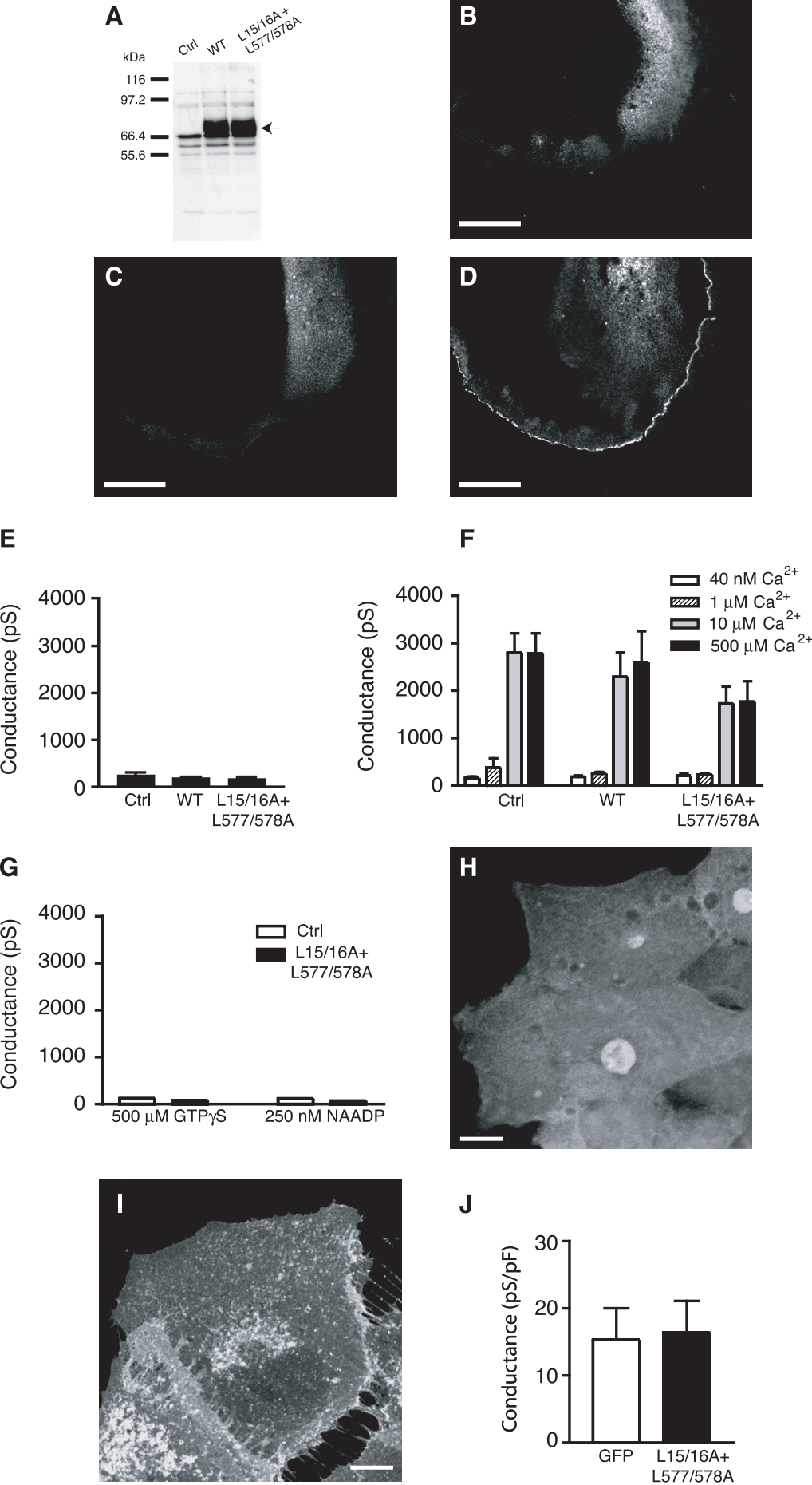
**CD8-mucolipin-1  
(L577/578A)**



**Lgp110**



**Supplementary Figure 1**



Supplementary Figure 2